Simultaneous Removal of NO₂ and C₆H₆ in an NO₂/C₆H₆ Mixture in Air by 172-nm Xe₂ Excimer Lamp at Atmospheric Pressure

Masaharu TSUJI[*1,2†] Takashi KAWAHARA[*3] Keiko UTO[*1]
Jun-Ichiro HAYASHI[*1,2] and Takeshi TSUJI[*4]
[†]E-mail of corresponding author: tsuji@cm.kyushu-u.ac.jp

NO₂ and C₆H₆ in an NO₂(200 ppm)/C₆H₆(200 ppm) mixture were simultaneously removed in air at atmospheric pressure using a 172-nm vacuum ultraviolet (VUV) Xe₂ excimer lamp. Reactants and products before and after photoirradiation were analyzed using an FTIR spectrometer. Results show that NO₂ and C₆H₆ were finally converted to HNO₃ and CO₂, respectively, by 172-nm photolysis of the NO₂/C₆H₆ mixture. Although the removal rate of NO₂ in the NO₂/C₆H₆ mixture was nearly the same as that of pure NO₂ in air, the C₆H₆ removal delayed until a sufficient reduction of NOx (NO₂, NO, and NO₃) concentrations. In order to obtain information on these results, computer simulation of decomposition processes was carried out. The delay of the C₆H₆ removal in the NO₂/C₆H₆ mixture was explained by 42–82 times larger reaction rate constants of the O(^{3}P) + NOx reactions than that of the O(^{3}P) + C₆H₆ reaction.

Key words: NOx, VOC, Excimer lamp, VUV photolysis, Air pollution

1. Introduction

Nitrogen oxides (NOx = NO + NO₂) and volatile organic compounds (VOCs) are major pollutants in the atmosphere, being a precursor to photochemical smog, acid rain, and ozone accumulation. The most general removal methods of NOx are based on catalytic reduction of NOx to elemental nitrogen by gaseous reducing agents, which are either selective (ammonia or ammonium compounds) or nonselective (NOx, carbon monoxide, and hydrocarbons).[1-3] In the selective catalytic reduction process, NOx is reduced by ammonia over a catalyst to form harmless N₂ and H₂O vapor without creating any secondary pollutants. Non-selective catalytic reduction requires injection of expensive NH₃ or other reducing agents without catalysts.

VOCs are recognized as major contributors to air pollution, either through their toxic nature or as participants in atmospheric photochemical reactions. They are emitted from different outdoor sources (motor vehicles, incomplete combustion in industrial processes) and from indoor sources.[4,5] Current methods to remove VOC from indoor air include plasma oxidation, photocatalytic oxidation, and adsorption by activated carbons.[6-12]

The plasma discharge method is also used in domestic air cleaners for NOx and VOC removal. Radicals formed by plasma discharge act as major active species for NOx and VOC removal.[13] However, these radicals also oxidize nitrogen and oxygen simultaneously, respectively generating NOx and ozone.[14] Therefore, the development of a new effective removal method of NOx and VOC is highly anticipated.

Vacuum ultraviolet (VUV) photolysis of air pollutants is a new promising method for NOx and VOC removal. Advantages of the VUV photolysis method are that it involves low-temperature operation in air at atmospheric pressure using a simple apparatus and no expensive catalysts. In general, when NOx and VOCs are decomposed using electric discharge in air, toxic NOx are formed because collisions of fast electrons generated in discharges with

*1 Institute for Materials Chemistry and Engineering, and Research and Education Center of Green Technology
*2 Department of Applied Science for Electronics and Materials
*3 Department of Applied Science for Electronics and Materials, Graduate Student
*4 Department of Materials Science, Shimane University

N_2 give active N atoms, which provide NOx by collisions with O_2. In this respect, an additional advantage of 172-nm photochemical method is that no NOx are emitted because active nitrogen is not generated under 172-nm photoirradiation of N_2.

　We have studied removal of such typical NOx and VOC as NO_2 and C_6H_6 in air using a side-on type of 172-nm excimer lamp.[15,16] NO_2 was dominantly converted to HNO_3 after photolysis, whereas C_6H_6 was converted to CO_2 via HCOOH and CO intermediates. Photochemical oxidants are the product of chemical reactions that occur between NOx and VOCs. Typical photochemical oxidants are ozone (O_3), hydrogen peroxide (H_2O_2), and peroxyacetyl nitrate (PAN). These photochemical oxidants are cause for concern, as they can have negative effects on human, plant, and animal health. Therefore, simultaneous removal techniques of NOx and VOCs in air at atmospheric conditions are required.

　In this study we attempted simultaneous removal of NO_2 and C_6H_6 in an NO_2/C_6H_6 mixture in air by 172-nm photolysis. Air dominantly consists of N_2(80%) and O_2(20%). Although 172-nm photons are not absorbed by N_2, they are absorbed by O_2 through Schumann–Runge continuum.[17] After photoabsorption, O_2 is selectively dissociated into the ground-state $O(^3P)$ atom and the metastable-state $O(^1D)$ atom: O_2 + hv (172 nm) → $O(^3P)$ + (^1D).[19] O_3 molecules are generated by the subsequent three-body reactions: $O(^3P)$ + O_2 + N_2 (or O_2) → O_3 + N_2 (or O_2). Therefore, in addition to direct VUV photodegradation, reactions of $O(^3P,^1D)$ and O_3 can participate in removal of an NO_2/C_6H_6 mixture. On the basis of our precious studies,[15,16] most important active species in the 172-nm photolysis of pure

NO_2 and C_6H_6 were found to be OH + NO_2 and $O(^3P)$ + C_6H_6 are major pathways for the formation of HNO_3 and CO_2 in the initial step. In the present study, removal mechanisms are discussed on the basis of computer simulation of reaction processes.

2.　Experimental

　Fig. 1 portrays a schematic diagram of side-on type of 172-nm excimer lamp used for this study. Table 1 presents the major performance of the side-on lamp (SL). The input power of the SL was 20 W. Experiments were conducted using the SL at a chamber volume of 235.5 cm^3 or 39.3 cm^3 where the chamber thicknesses was 3 cm or 0.5 cm, respectively.

　Light from an unfocused 172-nm Xe_2 lamp (155–200 nm range, UER20H172; Ushio Inc.) was irradiated into the photolysis chamber through a quartz window. Experiments were conducted using a closed batch chamber at atmospheric pressure. The concentration of NO_2 and C_6H_6 diluted in an N_2/O_2 mixture (20% O_2) was both 200 ppm (v/v). Outlet gases from the photolysis chamber were analyzed using a gas analysis system (FG122-LS; Horiba Ltd.) equipped with an FTIR spectrometer. The spectra in the 700–4000 cm^{-1} region were monitored. The concentrations of CO, CO_2, HCOOH, and NO_2 were calibrated using standard gases. On the other hand, the HNO_3, N_2O_5, and O_3 concentrations were evaluated by reference to standard spectral data supplied from Horiba Ltd. Thereby, the residual amounts of NO_2 and C_6H_6, C_t/C_0, were inferred from absorbance of FTIR peaks. Here, C_0 is the initial concentration of NO_2 or C_6H_6.

　The following gases were used: N_2 (purity >99.9998%; Taiyo Nippon Sanso (TNS) Corp.) O_2 (purity >99.99995%; TNS Corp.), NO_2 (2000 ppm in high-purity N_2; TNS Corp., and C_6H_6 (TNS.: 2000 ppm in high purity N_2). FTIR data indicated a small amount of H_2O (300 ppm) is
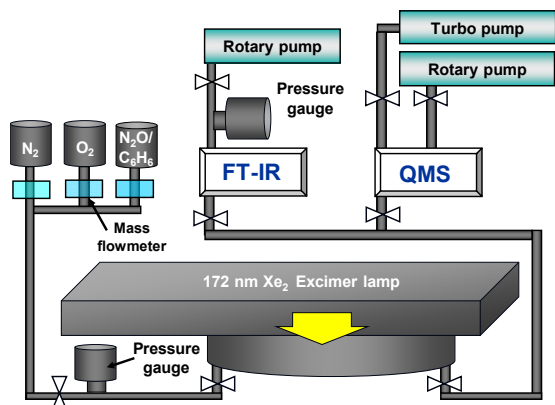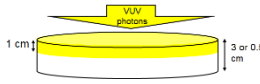

Fig. 1. Side-on type of 172-nm photolysis apparatus.

Table 1. Performance of photolysis chamber using a side-on lamp

VUV irradiation		
Input power		20 W
Irradiance		10 mW/cm^2
Window area		78.5 cm^2
Photon numbers/s		6.83×10^{17} photons/s
Chamber volume		235.5 or 39.3 cm^3

involved in the photolysis chamber as an impurity.

3. Results and discussion

3.1 Removal of NO_2 and C_6H_6 in an NO_2/C_6H_6 mixture by 172-nm photolysis in air

Fig. 2 shows FTIR spectra observed before and after 172-nm photolysis of an NO_2/C_6H_6 mixture in air (20% O_2) for 15 s at a chamber depth of 3 cm. Before photolysis, a strong NO_2 peak at about 1600 cm^{-1} and a weaker C_6H_6 peak at about 3200 cm^{-1} are observed. After 15 s photoirradiation, although the NO_2 peak disappears, the C_6H_6 peak becomes slightly weak. In addition, N_2O_5, HNO_3, $HCOOH$, CO, CO_2, and O_3 peaks appear. All of these product peaks have been observed by photolysis of either pure NO_2 or C_6H_6[15,16] so that no new product peaks, arising from the reactions between NO_2 and C_6H_6, were observed.

In Fig 3 is shown the dependence of concentrations of (a) NO_2 and C_6H_6, (b) $HCOOH$, CO, and CO_2, and (c) N_2O_5, HNO_3, and O_3 on the irradiation time. NO_2 is decomposed completely within 5 s, whereas the decomposition of C_6H_6 occurs more slowly and it takes about 50 s until its complete decomposition. The $HCOOH$ and CO concentrations have peaks at 50–60 s, whereas the CO_2 concentration increases with increasing the irradiation time. These results indicate that $HCOOH$ and CO intermediates are finally converted to CO_2. The N_2O_5 concentration has a peak at 5 s and decreases rapidly above that. On the other hand, the HNO_3 concentration increases until about 100 s and then levels off above thereafter. It is therefore reasonable to assume that N_2O_5 is efficiently converted to HNO_3 under our condition. The O_3 concentration increases from
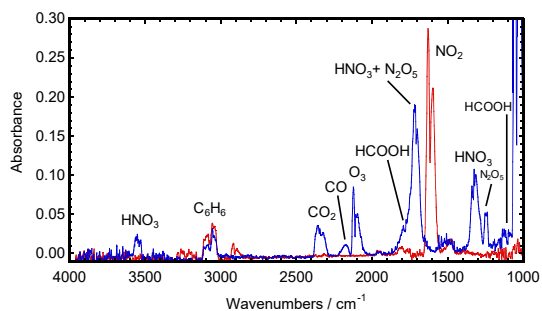
zero to 31,000 ppm with increasing the irradiation time from zero to 300 s.
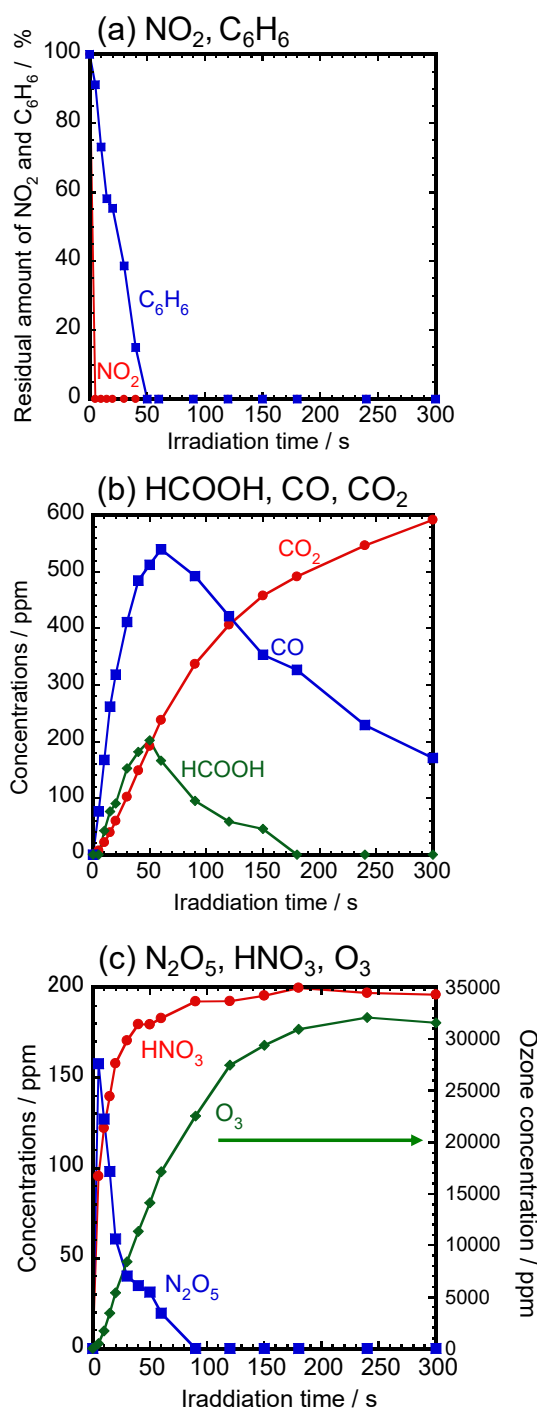

Fig. 3. Dependence of (a) residual amounts of NO_2 and C_6H_6, (b) concentrations of $HCOOH$, CO, and CO_2, and (c) concentrations of N_2O_5, HNO_3, and O_3 on the irradiation time in removal of NO_2 and C_6H_6 in an NO_2/C_6H_6 mixture by 172-nm excimer lamp in air (20% O_2). The chamber depth was 3 cm.
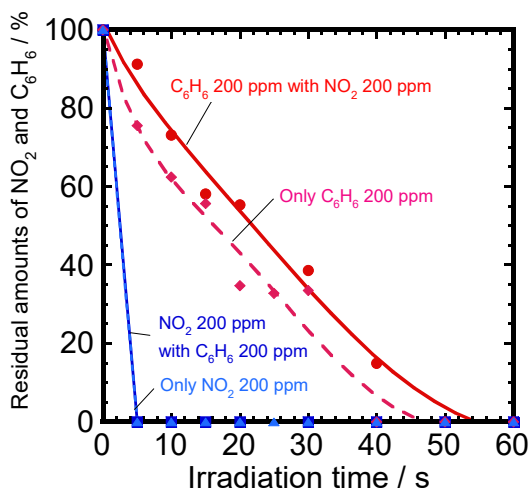

Fig. 2. FTIR spectra observed before (red line) and after 172-nm photolysis (blue line) of an NO_2/C_6H_6 mixture in air (20% O_2) for 15 s.

Fig. 4. Dependence of residual amounts of NO$_2$ and C$_6$H$_6$ on the irradiation time in pure NO$_2$ or C$_6$H$_6$ and NO$_2$/C$_6$H$_6$ mixture under 172-nm photolysis in air (20% O$_2$). The chamber depth was 3.0 cm.

In order to examine effects of mixing NO$_2$ with C$_6$H$_6$, dependence of residual amounts of NO$_2$ and C$_6$H$_6$ on the irradiation time in the NO$_2$/C$_6$H$_6$ mixture was compared with that in pure NO$_2$ and C$_6$H$_6$ (Fig. 4). It should be noted that the removal rate of NO$_2$ in the NO$_2$/C$_6$H$_6$ mixture is nearly identical to that of pure NO$_2$. On the other hand, the removal rate of C$_6$H$_6$ in the NO$_2$/C$_6$H$_6$ mixture is slower than that of pure C$_6$H$_6$, so that the removal curve of C$_6$H$_6$ in the NO$_2$/C$_6$H$_6$ mixture shifts to longer irradiation time in comparison with that of pure C$_6$H$_6$ by about 10 s.

3.2 Simulation of removal processes of NO$_2$ and C$_6$H$_6$ in an NO$_2$/C$_6$H$_6$ mixture by 172-nm photolysis in air

In our previous studies on 172-nm photolysis of pure NO$_2$ and C$_6$H$_6$, we succeeded in reproducing dependence of their removal amounts on the irradiation time by model calculations.[15,16] In this study, removal of an NO$_2$/C$_6$H$_6$ mixture is kinetically simulated by solving simultaneous differential equations using Runge–Kutta methods. Table A1 (Appendix) gives experimental parameters used for the simulation. For the simulation, we assumed that such active species as 172-nm photons, O(^{3}P), and O$_3$ were distributed uniformly within the reaction chamber. At a short chamber length of 0.5 cm, incident light is attenuated by only 7.23% at 20% O$_2$.[15,16] Therefore, we conducted removal experiments

of the NO$_2$/C$_6$H$_6$ mixture at 0.5 cm with a small reaction volume (39.3 mL), where the above assumption is expected to be well established. The obtained experimental data for NO$_2$, C$_6$H$_6$, and HNO$_3$ are presented in Fig. 5(a). The concentration of NO$_2$ decreases to zero below 5 s, whereas that of C$_6$H$_6$ decreases to zero at 10 s. The HNO$_3$ concentration increases from zero to about 200 ppm after about 30 s.

Table 2 shows elementary reactions used for the simulation. They consist of 172-nm photolysis of O$_2$ leading to O(^{1}D) + O(^{3}P) atoms (1),[18] relaxation of O(^{1}D) to O(^{3}P) (2a)–(2b), three-body reactions leading to O$_3$ (3a)–(3b), VUV photolysis of O$_3$ (4a)–(4b), dissociation of O$_3$ (5)–(7), three-body recombination of O(^{3}P) (8a)–(8b), VUV photolysis of NO$_2$, (9), NOx + O$_3$ reactions (10)–(12), NOx + O(^{3}P) reactions (13)–(17), other NOx reactions (18)–(21), and
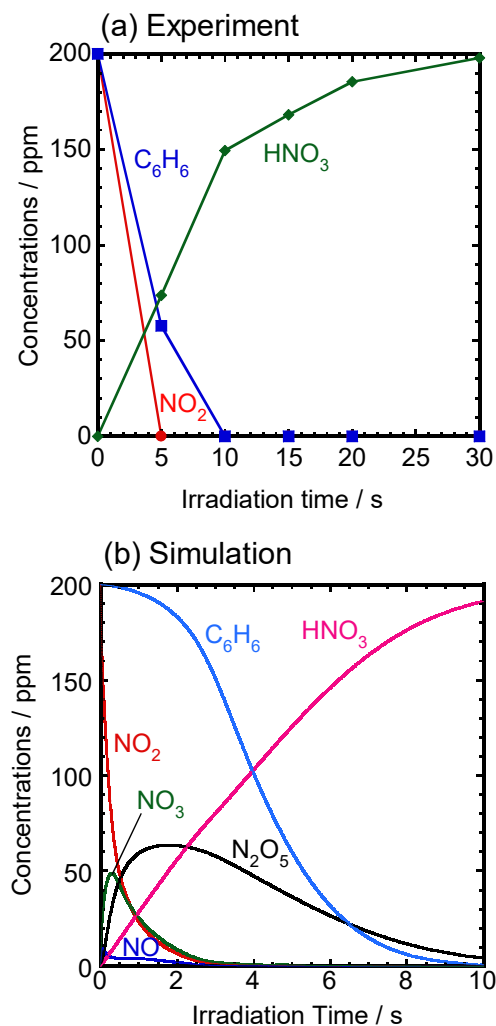

Fig. 5. Dependence of reagents and products on the irradiation time obtained by (a) experiment and (b) simulation. The chamber depth was 0.5 cm.
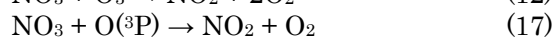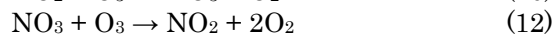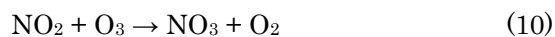
Table 2

Reactions considered for the simulation of simultaneous removal of NO_2 and C_6H_6 in the NO_2/C_6H_6 mixture by 172-nm photolysis in air.

| Chemical equations		
$O_2 + h\nu \rightarrow O(^3P) + O(^1D)$	σ_1	(1)
$O(^1D) + O_2 \rightarrow O(^3P) + O_2$	k_{2a}	(2a)
$O(^1D) + N_2 \rightarrow O(^3P) + N_2$	k_{2b}	(2b)
$O(^3P) + O_2 + O_2 \rightarrow O_3 + O_2$	k_{3a}	(3a)
$O(^3P) + O_2 + N_2 \rightarrow O_3 + N_2$	k_{3b}	(3b)
$O_3 + h\nu \rightarrow O(^3P) + O_2$	σ_{4a}	(4a)
$O_3 + h\nu \rightarrow 3O(^3P)$	σ_{4b}	(4b)
$O_3 \rightarrow O_2 + O(^3P)$	k_5	(5)
$O_3 + O_3 \rightarrow 3O_2$	k_6	(6)
$O(^3P) + O_3 \rightarrow 2O_2$	k_7	(7)
$2O(^3P) + O_2 \rightarrow O_2 + O_2$	k_{8a}	(8a)
$2O(^3P) + N_2 \rightarrow O_2 + N_2$	k_{8b}	(8b)
$NO_2 + h\nu \rightarrow NO + O(^3P)$	σ_9	(9)
$NO_2 + O_3 \rightarrow NO_3 + O_2$	k_{10}	(10)
$NO + O_3 \rightarrow NO_2 + O_2$	k_{11}	(11)
$NO_3 + O_3 \rightarrow NO_2 + 2O_2$	k_{12}	(12)
$NO_2 + O(^3P) \rightarrow NO_3$	k_{13}	(13)
$NO_2 + O(^3P) + N_2$ $\rightarrow NO_3 + N_2$	k_{14a}	(14a)
$NO_2 + O(^3P) + O_2$ $\rightarrow NO_3 + O_2$	k_{14b}	(14b)
$NO_2 + O(^3P) \rightarrow NO + O_2$	k_{15}	(15)
$NO + O(^3P) \rightarrow NO_2$	k_{16}	(16)
$NO_3 + O(^3P) \rightarrow NO_2 + O_2$	k_{17}	(17)
$NO_2 + NO_3 \rightarrow N_2O_5$	k_{18}	(18)
$NO_2 + NO_3$ $\rightarrow NO + NO_2 + O_2$	k_{19}	(19)
$NO + NO_3 \rightarrow 2NO_2$	k_{20}	(20)
$N_2O_5 + H_2O \rightarrow 2HNO_3$	k_{21}	(21)
$H_2O + h\nu \rightarrow OH + O(^3P)$	σ_{22}	(22)
$NO_2 + OH \rightarrow HNO_3$	k_{23}	(23)
$2N_2O_5 \rightarrow 4NO_2 + O_2$	k_{24}	(24)
$N_2O_5 + O(^3P) \rightarrow 2NO_2 + O_2$	k_{25}	(25)
$C_6H_6 + h\nu \rightarrow$ products	σ_{26}	(26)
$O(^3P) + C_6H_6 \rightarrow$ Products	k_{27}	(27)
$O_3 + C_6H_6 \rightarrow$ Products	k_{28}	(28)

VUV photolysis of H_2O (22), and other NOx reactions (23)–(25). 172-nm photolysis of C_6H_6 (26) and reactions of C_6H_6 (27)–(28) were also considered.

In the simulation, we used the same reaction rate constants and spectroscopic data as those used in our previous studies.[15,16] Most of kinetic and spectroscopic data were obtained from Refs. 17–19. The temperature rise of 0.026 K/s in the photolysis chamber after photoirradiation was assumed for the simulation of simultaneous removal of NO_2 and C_6H_6 in the NO_2/C_6H_6 mixture because the temperature of the reaction chamber increases concomitantly with increasing photoirradiation time. The validity of this assumption was confirmed from the time evolution of O_3 in air in our photolysis chamber.[15] Fig. 5(b) shows simulation data for NO_2, NO, NO_3, N_2O_5, HNO_3, and C_6H_6 in the NO_2/C_6H_6 mixture.

In our removal model of NO_2, NO_2 molecules are oxidized to NO_3 by collisions with O_3, whereas NO_3 molecules are reduced to NO_2 by collisions with O_3 and $O(^3P)$.

$$NO_2 + O_3 \rightarrow NO_3 + O_2 \qquad (10)$$
$$NO_3 + O_3 \rightarrow NO_2 + 2O_2 \qquad (12)$$
$$NO_3 + O(^3P) \rightarrow NO_2 + O_2 \qquad (17)$$

N_2O_5 molecules are formed by the $NO_2 + NO_3$ reaction.

$$NO_2 + NO_3 \rightarrow N_2O_5 \qquad (18)$$
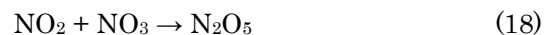
It was further converted to HNO_3 by the $N_2O_5 + H_2O$ reaction.

$$N_2O_5 + H_2O \rightarrow 2HNO_3 \qquad (21)$$

In addition, reactions of OH radicals, formed by 172-nm photolysis of H_2O, are considered.

$$H_2O + h\nu \ (172 \ nm) \rightarrow OH + H \qquad (22)$$
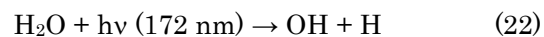
The $NO_2 + OH$ reaction gives HNO_3.

$$NO_2 + OH \rightarrow HNO_3 \qquad (23)$$

N_2O_5 formed by the oxidation of NO_2 is reduced again to NO_2 by the first-order reaction.

$$2N_2O_5 \rightarrow 4NO_2 + O_2 \qquad (24)$$
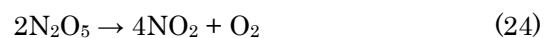
N_2O_5 is also decomposed by the reaction with $O(^3P)$.
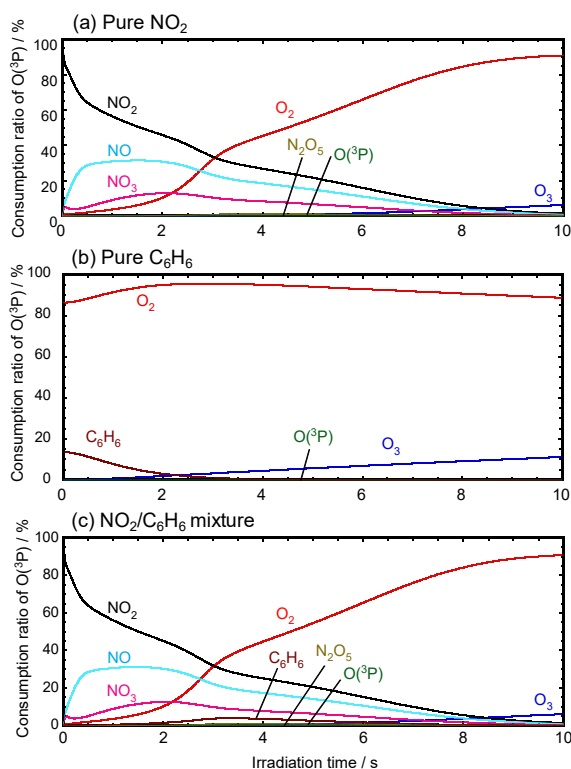
Fig. 6. Dependence of consumption ratio of O(^{3}P) in (a) pure NO$_2$, (b) pure C$_6$H$_6$, and (c) NO$_2$/C$_6$H$_6$ mixture on the irradiation time under 172-nm photolysis. Data were obtained by model calculations. The chamber depth was 0.5 cm.

$$N_2O_5 + O(^3P) \rightarrow 2NO_2 + O_2 \qquad (25)$$
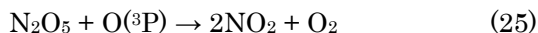
In our removal model for the NO$_2$/C$_6$H$_6$ mixture (Fig. 5(b)), NO$_2$ is decomposed below about 3 s. NO$_3$ and NO are formed below 2 s and disappear at about 3 s. The N$_2$O$_5$ concentration increases to about 60 ppm at about 2 s and decreases to 4 ppm at 10 s. On the other hand, the concentration of HNO$_3$, which is the dominant product in this model, increases gradually from zero to 190 ppm until 10 s. A reasonable agreement is found between the calculated and experimental data for time profiles of the NO$_2$, HNO$_3$, and N$_2$O$_5$ concentrations, indicating that NO$_2$ removal proceeds dominantly through our proposed removal model.

Fig. 5(b) also shows removal profile of C$_6$H$_6$ calculated taking account of all reactions processes given in Table 2. In our removal model of C$_6$H$_6$, C$_6$H$_6$ molecules are decomposed by the O(^{3}P) + C$_6$H$_6$ reaction. A satisfactory agreement between the experimental and simulation data is obtained for the C$_6$H$_6$ removal in the NO$_2$/C$_6$H$_6$ mixture, implying

that our simulation model is applicable to reproduce the removal profile of C$_6$H$_6$ in the NO$_2$/C$_6$H$_6$ mixture

Fig. 6 shows the dependence of the consumption ratio of O(^{3}P) on the irradiation time in pure NO$_2$ or C$_6$H$_6$, and NO$_2$/C$_6$H$_6$ mixture obtained by simulations. Results show that the time profile of consumption ratio of O(^{3}P) obtained from the NO$_2$/C$_6$H$_6$ mixture is nearly identical to that obtained from pure NO$_2$, excpet for the time profile of consumption ratio of O(^{3}P) by C$_6$H$_6$. Below about 3 s, O(^{3}P) atoms are dominantly consumed by NO$_2$, NO, and NO$_3$. Although the consumption ratio of O(^{3}P) by O$_2$ is small below 2 s, it gradually increases above 2 s and it becomes larger than those of NO$_2$, NO, and NO$_3$ above about 3 s.

It should be noted that the time profile of consumption ratio of O(^{3}P) by C$_6$H$_6$ in the NO$_2$/C$_6$H$_6$ mixture is different from that in pure C$_6$H$_6$. The consumption ratio of the O(^{3}P) + C$_6$H$_6$ reaction rapidly decreases from 14% to 1.1% in the short 0–3 s range in pure C$_6$H$_6$, whereas it occupies only 1.5–4.0 % in the 2–6 s range in the NO$_2$/C$_6$H$_6$ mixture. On the basis of above facts, O(^{3}P) atoms are initially consumed by NOx in the NO$_2$/C$_6$H$_6$ mixture, so that the consumption of O(^{3}P) by C$_6$H$_6$ delays by 4±2 s in the NO$_2$/C$_6$H$_6$ mixture.

We discuss below the reason why the time profile of consumption ratio of O(^{3}P) by C$_6$H$_6$ in the NO$_2$/C$_6$H$_6$ mixture is different from that in pure C$_6$H$_6$ using known reaction rate constants of related reactions. Removal of NO$_2$ and C$_6$H$_6$ occurs competitively in the NO$_2$/C$_6$H$_6$ mixture. The reaction rate constant of the O(^{3}P) + C$_6$H$_6$ reaction (k_{27} = 4.04 ×10^{-14} cm^3 s^{-1} molecule^{-1}) is smaller than those of the O(^{3}P) + NO$_2$ reactions (k_{13} + k_{15} = 3.33 ×10^{-11} cm^3 s^{-1} molecule^{-1}) by a factor of 82.[19] It is also smaller than those of the O(^{3}P) + NO reaction (k_{16} = 2.99 ×10^{-11} cm^3 s^{-1} molecule^{-1}) and O(^{3}P) + NO$_3$ reaction (k_{17} = 1.70 ×10^{-11} cm^3 s^{-1} molecule^{-1}) by factors of 74 and 42, respectively.[19] Therefore, O(^{3}P) atoms are initially consumed by reactions with such NOx as NO$_2$, NO, and NO$_3$. The O(^{3}P) + C$_6$H$_6$ reaction occurs after the NO$_2$, NO, and NO$_3$ concentrations become low, where the initial NO$_2$ concentration is reduced to about half. The consumption of O(^{3}P) by NOx in the initial stage is attributed to the main reason why the C$_6$H$_6$ removal delayed until a sufficient reduction of NOx.

For the practical use of our removal method, a flow system, by which continuous removal of NO$_2$/C$_6$H$_6$ is possible, is required. On the basis of the present results, a long reaction chamber

is necessary for the simultaneous removal of NO_2 and C_6H_6 in the NO_2/C_6H_6 mixture using a flow system, where NO_2 must be removed to some extent upstream and the C_6H_6 is removed downstream at low NO_2 concentrations.

4.　Summary and Conclusion

　　NO_2 and C_6H_6 in an NO_2/C_6H_6 mixture were simultaneously removed in air at atmospheric pressure using a 172-nm Xe_2 excimer lamp. Reactants and products before and after photoirradiation demonstrated that NO_2 and C_6H_6 were finally converted to HNO_3 and CO_2, respectively. Although the removal rate of NO_2 in the NO_2/C_6H_6 mixture was nearly the same as that of pure NO_2 in air, the C_6H_6 removal delayed until the NO_2 concentration is reduced to about half. In order to obtain information on these results, computer simulation of removal processes of NO_2 and C_6H_6 in the NO_2/C_6H_6 mixture was carried out. The delay of the C_6H_6 removal in the NO_2/C_6H_6 mixture was explained by much larger reaction rate constants of the $O(^3P) + NOx$ reactions than that of the $O(^3P) + C_6H_6$ reaction. The present results give fundamental information on the development of photochemical removal apparatus of mixtures of NOx/VOC.

References

1)　M. Devadas, O. Krocher, M. Elsener, A. Wokaun, N. Soger, M. Pfeifer, and Y. Demel, *Appl. Catal. B Environ.,* 67, 187 (2006).
2)　R. M. Heck, R. J. Farrauto, and S. T. Gulati, Catalytic air pollution control: commercial technology, Vol. 522. (2009). Wiley, Hoboken.
3)　T. Ye, D. Chen, Y. Yin, J. Liu, and X. Zeng, *Catalysts*, 7, 258 (2017).
4)　R. Pal, K. H. Kim, Y. J. Hong, and E. C. Jeon, *J. Hazard. Mater.*, 153, 1122 (2008).
5)　D. A. Sarigiannis, S. P. Karakitsios, A. Gotti, I. L. Liakos, and A. Katsoyiannis, *Environ. Int.*, 37, 743 (2011).
6)　M. Balcerek, K. Pielech-Przybylska, P. Patelski, U. Dziekońska-Kubczak, and T. Jusel, *Food. Addit. Contam. Part A*, 34, 714 (2017).
7)　H. L. Chen, J. M. Lee, S. H. Chen, M. B. Chang, S. J. Yu, and S. N. Li, *Environ. Sci. Technol.*, 43, 2216 (2009).
8)　Y. El-Sayed and T. J. Bandosz, *Langmuir*, 18, 3213 (2002).
9)　T. Hayashi, M. Kumita, and Y. Otani, *Environ. Sci. Technol.*, 39, 5436 (2005).
10)　J. H. Mo, Y. P. Zhang, Q. Xu, J. J. Lamson, and R. Zhao, *Atmos. Environ.*, 43, 2229 (2009).
11)　M. Tomatis, H. H. Xu, J. He, and X. D. Zhang, *J. Chem.*, 8324826 (2016).
12)　A. M. Vandenbroucke, R. Morent, N. De Geyter, and C. Leys, *J. Hazard. Mater.*, 195, 30. (2011).
13)　M. Okubo, T. Yamamoto, T. Kuroki, and H. Fukumoto, *IEEE Trans. Ind. Appl.*, 37, 1505 (2001).
14)　N. Sano, T. Nagamoto, H. Tamon, T. Suzuki, and M. Okazaki, *Ind. Eng. Chem. Res.*, 36, 3783 (1997).
15)　M. Tsuji, T. Kawahara, K. Uto, N. Kamo, M. Miyano, J.-I. Hayashi, and T. Tsuji, *Environ. Sci. Pollut. Res.*, 25, 18980 (2018).
16)　M. Tsuji, T. Kawahara, K. Uto, J.-I. Hayashi, and T. Tsuji, *Int. J. Environ. Sci. Technol.*, in press (2019). https://doi.org/10.1007/s13762-018-2131-y.
17)　H. Okabe, Photochemistry of small molecules, Wiley, New York (1978).
18)　J. B. Nee and P. C. Lee, *J. Phys. Chem. A*, 101, 6653 (1997).
19)　R. Atkinson, D. L. Baulch, R. A. Cox, R. F. Hampson Jr, J. A. Kerr, M. J. Rossi, and J. Troe, *J. Phys. Chem. Ref. Data,* 26, 1329 (1997). Updated data were obtained from NIST Chemical Kinetics Database on the Web, Standard Reference Database 17, Version 7.0 (Web Version), Release 1.6.8, Data Version 2017.07. http://kinetics.nist.gov/kinetics/index.jsp

Appendix

Table A1.　Parameters used for the simulation of simultaneous removal of NO_2 and C_6H_6 in the NO_2/C_6H_6 mixture by 172-nm photolysis in air.

Absorption cross section of O_2 at 172 nm	$\sigma_1 = 4.63 \times 10^{-19}$ [cm^2/molecule]
Absorption cross section of O_3 at 172 nm	$\sigma_4 = 8.16 \times 10^{-19}$ [cm^2/molecule]
Branching fraction of photolysis of O_3 at 172 nm $O_3 + h\nu$ $\quad \to \; O(^3P) + O_2$ (4a) $\quad \to \; 3O(^3P) \quad$ (4b)	4a : 4b = 0.9 : 0.1
Absorption cross section of NO_2 at 172 nm	$\sigma_9 = 1.45 \times 10^{-17}$ [cm^2/molecule]
Absorption cross section of C_6H_6 at 172 nm	$\sigma_{26} = 6.48 \times 10^{-21}$ [cm^2/molecule]
Absorption cross section of H_2O at 172 nm	$\sigma_{22} = 8.16 \times 10^{-19}$ [cm^2/molecule]
Initial reaction temperature	297.6 [K]
Initial concentration of N_2	80 [%]
Initial concentration of O_2	20 [%]
Initial concentration of C_6H_6	200 [ppm]
Initial concentration of NO_2	200 [ppm]
Initial concentration of H_2O	300 [ppm]
The number of repetitions per sec	1000 [times/s]